34th Annual International Conference of the IEEE EMBS
San Diego, California USA, 28 August - 1 September, 2012

Stretchable Biocompatible Electronics by Embedding Electrical Circuitry in Biocompatible Elastomers

Amir Jahanshahi [1] and Pietro Salvo [1] and Jan Vanfleteren [1]

***Abstract*— Stretchable and curvilinear electronics has been used recently for the fabrication of micro systems interacting with the human body. The applications range from different kinds of implantable sensors inside the body to conformable electrodes and artificial skins. One of the key parameters in biocompatible stretchable electronics is the fabrication of reliable electrical interconnects. Although very recent literature has reported on the reliability of stretchable interconnects by cyclic loading, work still needs to be done on the integration of electrical circuitry composed of rigid components and stretchable interconnects in a biological environment. In this work, the feasibility of a developed technology to fabricate simple electrical circuits with meander shaped stretchable interconnects is presented. Stretchable interconnects are 200 nm thin Au layer supported with polyimide (PI). A stretchable array of light emitting diodes (LEDs) is embedded in biocompatible elastomer using this technology platform and it features a 50 % total elongation.**

I. INTRODUCTION

Curvilinear and stretchable electronics has received a remarkable attention in recent years as it can be observed by the number of publications. There are excellent reviews available in the literature on the applications [1], [2].

This emerging field has opened the doors to the vast bio related systems and devices. In particular, as soon as the electronics becomes conformable, it can be applied comfortably to the skin as a curvilinear surface, implanted inside the body to deliver the drugs and other emerging applications. Namely, artificial skin [3], [4], electronic eye camera [5] and textiles in the context of wearable electronics [6] have been successfully fabricated.

In general a marriage between reliable electronics and biocompatibility is demanded in order for the device to have interaction with the body. Although depending on the type of applications, e.g., in-vivo, in-vitro or physical conditions, the proportions are different. Carbon nano tube based stretchable interconnects are used successfully in a number of applications such as conformal sensors [7], but, up to now no promising value is reported for their cycling reliabilities. In contrast, metal interconnects in elastomers have shown remarkable cycling reliabilities in very recent literature [8], [9], [10], [11]. In [10] a detailed comparison between the mentioned references is provided.

Moreover, in [10], we reported the fabrication and the cyclic reliability results of single track (ST) and multi track (MT) meander shaped Au interconnects. In this article, the application of the proposed technology on embedding the electronic circuitry is presented. As a prototype, a stretchable array of light emitting diodes (LEDs) is fabricated and embedded in the bio compatible elastomer. The effect of the interconnect type on the maximum elongation is also discussed. The relatively high 50 % elongation of the array shows the feasibility of the process in integration of electrical circuitry in the field of stretchable and curvilinear electronics.

II. FABRICATION

The complete schematic diagram of the fabrication is illustrated in Fig. 1. Fabrication starts on a double-sided

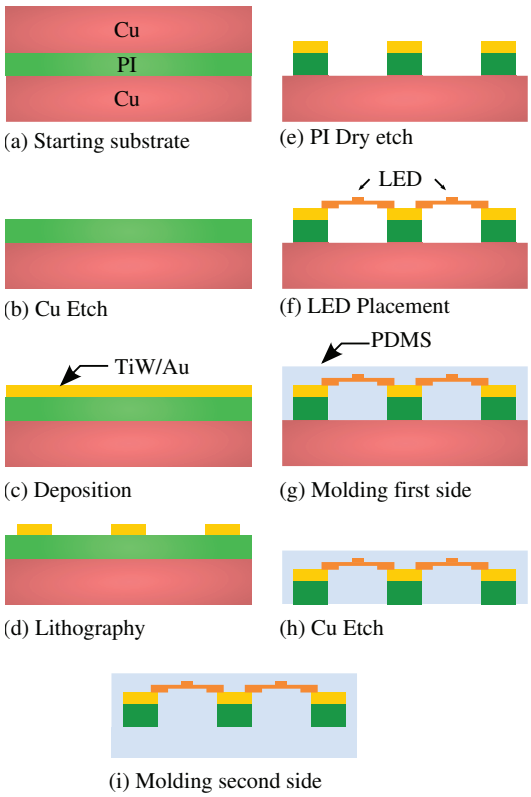

Fig. 1: Complete Fabricatin Process: (a) Pyralux® AP 7412 substrate is illustrated. (b) One Cu layer is etched away while protecting the other layer with a tape. (c) TiW/Au is sputter coated on the PI. (d) Au/TiW is patterned via standard photolithography. (e) PI is dry etched in an RIE. (f) LED is mounted on the gold pads using conductive glue. (g) Top side of the sample is cast in biocompatible PDMS. (h) Cu layer is wet etched. (i) The second side of the sample is also cast in PDMS.

*This work is granted through an IMEC PhD scholarship.

[1]We are all with the Centre for Microsystems Technology (CMST), IMEC–Ghent University, Technologiepark 914a, B-9052 Ghent, Belgium. Jan.Vanfleteren@elis.ugent.be

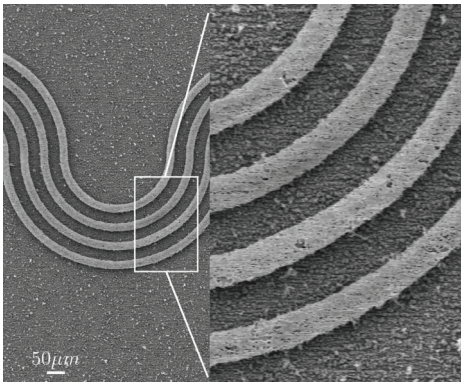

Fig. 2: An SEM micrograph of MT meanders showing the 12 µm thick Au/PI meanders on Cu foil.

commercial flex substrate (Pyralux® AP 7412 by Dupont™) composed of Cu/PI/Cu, where Cu and PI are 18 µm and 12 µm thick, respectively (Fig. 1a). One of the Cu layers is wet etched using a spray etcher while protecting the other Cu layer with a paste tape (Fig. 1b). 50 nm of TiW, followed by 200 nm of Au, are sputter coated on the PI (Fig. 1c). TiW behaves as an excellent intermediate layer between PI and Au for adhesion purposes. The next step is photolithography of TiW/Au to transfer the electrical patterns including the LED pads and the meander shaped tracks connecting the active areas (Fig. 1d). In the following step, the PI is dry etched in a reactive ion etching (RIE) system for 75 min (Fig. 1e). Following the PI etching, LEDs can be mounted on the designated pads using the conductive glue CE3103® by Emerson™ (Fig. 1f). The LEDs are purchased from Farnell™ and have the standard 0805 surface mount footprint. At this stage, the external wires are also attached to the terminal pads using the same conductive glue. The conductive glue is cured in a convection oven at 120 °C for 15 min. The next step is the injection molding of PDMS on top side of the sample (Fig. 1g). Nusil™ MED® 6010 implantation grade PDMS is cast in a PMMA mold in order to provide the biocompatibility requirements of the fabricated structure. PDMS is cured overnight in a convection oven at 60 °C. Then, the Cu foil from the back side of the sample is wet etched in a CuCl2 solution (Fig. 1h). The cured PDMS and the PI are excellent protective layers for the tracks, LEDs and the wires from the etching solution. The fabrication process is completed by injection molding the back side of the sample with the same conditions used for the top side (Fig. 1i).

An SEM micrograph of multi-track (MT) meanders when the sample is still on Cu-foil, i.e., at the stage illustrated by Fig. 1e, is shown in Fig. 2. The rough surface of Cu-foil and the porous Au layer on top are visible.

III. Results and Discussion

In each sample an array of 4 × 5 LEDs is fabricated as illustrated in Fig. 3. As can be seen, all the LEDs are electrically connected in parallel in a way to be powered from only two terminals on the opposite ends of the sample.

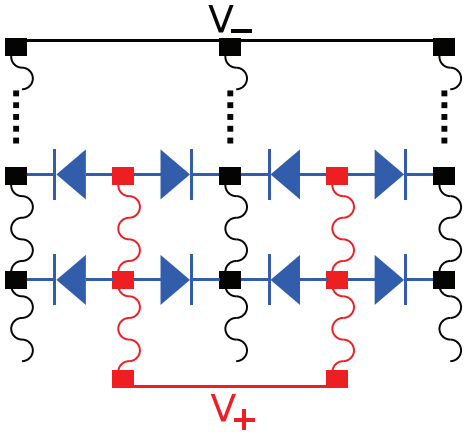

Fig. 3: Schematic diagram of the electrically parallel design of the LED array.

In order to investigate the performance of single-track (ST) and narrow multi track (MT) designs for interconnecting the active areas in a stretchable environment, both MT and ST stretchable LED arrays are fabricated. The fabrication is done using the same set of parameters except the lithography mask which is used for pattering the TiW/Au (Fig. 1d).

For illustration purposes, a microscope image of the MT

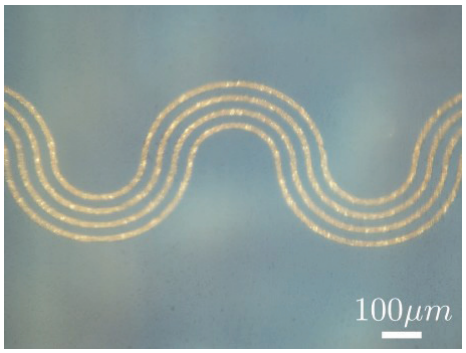

(a) MT

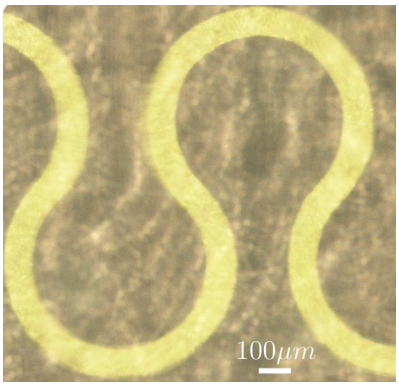

(b) ST

Fig. 4: Optical microscope images of the fabricated (a) MT and (b) ST meanders are shown. The hazy background is due to the fact that the tracks are embedded in PDMS.

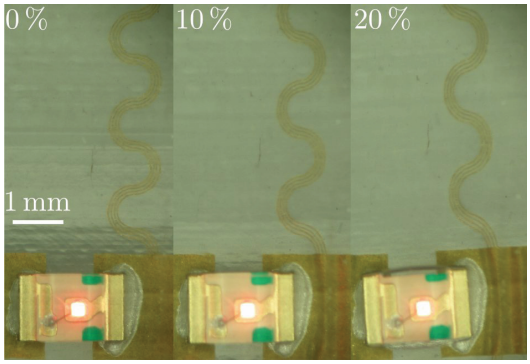

Fig. 5: Optical microscope images of one LED with its interconnecting MT meander is shown at zero to 20 % elongations.

and ST design is shown in Fig. 4a and Fig. 4b, respectively. Both tracks are embedded in PDMS and the images are captured using a polarizer filter. In this work, elongation is based on the engineering strain definition $\varepsilon = (L_1 - L_0)/L_0$, where L_0 and L_1 are the initial length and final length of the sample, respectively. In this work, track width is represented by w and the distance between tracks in MT design is represented by d. Form factor (F) is defined as the radius of inner track over w. The sample is mounted in a PMMA clamp and elongated precisely using an Instron^{TM}-5543.

A. *MT* ($w = 30\,\mu$m, $d = 30\,\mu$m, $F10$)

In a previous work [10], it is shown that narrow MT design outperforms thicker ST design in terms of resistance variation of the tracks. The MT ($w = 20\,\mu$m, $d = 20\,\mu$m) tracks show nearly no change in resistance over 200 k cycles at 40 % elongation, whereas ST ($w = 100\,\mu$m) resistance increases more than 70 %. When there is only meander-shaped track in the stretchable environment, the failure mechanism is governed by the crack propagation in individual tracks. By lowering the width, the overall stress is minimized, thus reducing the crack propagation rate. However by integrating the LEDs as the active area in the stretchable environment, the mechanism of failure changes from crack propagation to rigid-flexible boundary interface. In this case, the 2 mm × 4 mm region formed by the LED and the pad area can be considered rigid compared to the much smaller 30 µm width tracks. Therefore, relatively high stress is introduced just in the boundary of the track with the pad

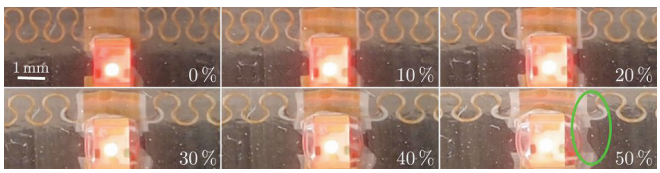

Fig. 6: Optical microscope images of one LED with its interconnecting ST meander is shown at zero to 50 % elongations. The green circled area shows clearly the buckled Au layer. This buckling is also visible at smaller elongations.

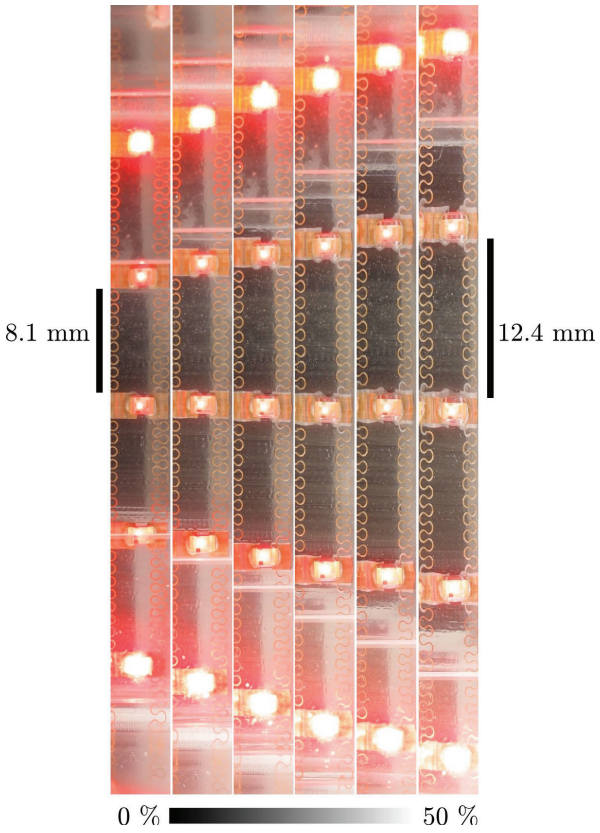

Fig. 7: Camera images of one line of the sample demonstrating the total stretchability of the array. The middle LED has the least light intensity because of resistive voltage drop on the stretchable meanders.

and the track can only withstand it for smaller elongations. Fig. 5 shows an image of one LED and the MT interconnects, which are elongated for a maximum of 20 %. The maximum elongation achieved in this design is approximately 22 % before electrical connection is lost and the LED turns off. The relatively high stress can be seen by the visible wrinkles in the pad area at 10 % and 20 % elongations. Because of the 2 mm thick PDMS on top of the tracks, the failure point can not be observed by optical inspection. However, it is believed that it is created in the interface. This hypothesis is also supported in other works in the literature [9].

B. *ST*($w = 100\,\mu$m, $F3$)

When the track width grows in ST design, although the stress in the track itself increases, the relative stress at the rigid-flexible interface decreases compared to the narrow MT design.

Fig. 6 shows a zoom picture of ST design with a maximum elongation of 50 %. The extremely high stress near the interface of the pad is indicated with a green circle in the 50 % elongation image. It can be seen that the track is completely buckled from its position, while still electrically conducting. Starting from 20 %, the buckling of the pad from the white region around it also becomes visible. Fig. 7 shows a complete camera image of one line of the LED

array at different elongation values. The difference in the light intensity is only due to the parallel design and the non-zero resistance interconnects between the LEDs. In fact, the closest LEDs to the power source, i.e., the first and the last one, limit the voltage. The voltage is dropped over the interconnect resistance and reaches its minimum in vicinity of the middle LED, which has thus the lowest intensity.

Another notable point in Fig. 7 is the effect of Poissons ratio. As the elongation is increased, the distance between the two parallel tracks is remarkably decreased which illustrates the transverse strain in the sample. This source of strain is added to the total strain in the sample, particularly when either the sample is narrow or the track is near the edge.

IV. Conclusion

An LED array is presented as a prototype to demonstrate the electrical circuit integration in biocompatible elastomers using our developed fabrication process. The proposed fabrication process can be carried out with any arbitrary pattern in order to transfer any kind of circuitry on the surface. It has to be noted that the high temperature needed for curing the conductive glue at 120 °C, although can be decreased by using a different glue, does not hamper electronic performance of the components commercially available, either packaged or bared die version. The authors believe that the method provided in this article is a promising technique towards realization of biocompatible stretchable electronics that can be used in potential applications including in-vivo and in-vitro drug delivery, artificial skin electrodes and physical sensors interacting with the muscles and moving organs of the body.

References

[1] D. J. Lipomi and Z. Bao, "Stretchable, elastic materials and devices for solar energy conversion," *Energy Environ. Sci.*, vol. 4, pp. 3314–3328, 2011.

[2] J. A. Rogers, T. Someya, and Y. Huang, "Materials and mechanics for stretchable electronics," *Science*, vol. 327, no. 5973, pp. 1603–1607, 2010.

[3] D. Cotton, I. Graz, and S. Lacour, "A multifunctional capacitive sensor for stretchable electronic skins," *Sensors Journal, IEEE*, vol. 9, no. 12, pp. 2008 –2009, 2009.

[4] M.-Y. Cheng, C.-M. Tsao, Y.-Z. Lai, and Y.-J. Yang, "The development of a highly twistable tactile sensing array with stretchable helical electrodes," *Sensors and Actuators A: Physical*, vol. 166, no. 2, pp. 226 – 233, 2011.

[5] H. C. Ko, M. P. Stoykovich, J. Song, V. Malyarchuk, W. M. Choi, C.-J. Yu, J. B. Geddes III, J. Xiao, S. Wang, Y. Huang, and J. A. Rogers, "A hemispherical electronic eye camera based on compressible silicon optoelectronics," *Nature*, vol. 454, no. 7205, pp. 748–753, 2008.

[6] L. Hu, M. Pasta, F. L. Mantia, L. Cui, S. Jeong, H. D. Deshazer, J. W. Choi, S. M. Han, and Y. Cui, "Stretchable, porous, and conductive energy textiles," *Nano Letters*, vol. 10, no. 2, pp. 708–714, 2010.

[7] T. Takahashi, K. Takei, A. G. Gillies, R. S. Fearing, and A. Javey, "Carbon nanotube active-matrix backplanes for conformal electronics and sensors," *Nano Letters*, vol. 11, no. 12, pp. 5408–5413, 2011.

[8] G. Corbelli, C. Ghisleri, M. Marelli, P. Milani, and L. Ravagnan, "Highly deformable nanostructured elastomeric electrodes with improving conductivity upon cyclical stretching," *Advanced Materials*, vol. 23, no. 39, pp. 4504–4508, 2011.

[9] X. Hu, P. Krull, B. de Graff, K. Dowling, J. A. Rogers, and W. J. Arora, "Stretchable inorganic-semiconductor electronic systems," *Advanced Materials*, vol. 23, no. 26, pp. 2933–2936, 2011.

[10] A. Jahanshahi, P. Salvo, and J. Vanfleteren, "On reliable stretchable gold interconnects in biocompatible elastomers," *Journal of Polymer Science Part B: Polymer Physics*, p. To appear, 2012.

[11] R. Verplancke, F. Bossuyt, D. Cuypers, and J. Vanfleteren, "Thin-film stretchable electronics technology based on meandering interconnections: fabrication and mechanical performance," *Journal of Micromechanics and Microengineering*, vol. 22, no. 1, p. 015002, 2012.